PERGAMON

International Journal of Heat and Mass Transfer 44 (2001) 2699–2710

International Journal of HEAT and MASS TRANSFER

www.elsevier.com/locate/ijhmt

Bubble growth in a uniform and spatially distributed temperature field

A.J. Robinson, R.L. Judd *

Department of Mechanical Engineering, McMaster University, Hamilton, Ont. L8S 4L7, Canada

Received 29 February 2000; received in revised form 8 September 2000

Abstract

A theory has been developed which has been shown to predict experimental bubble growth data for both spherical growth in an unbounded liquid and hemispherical growth at a heated plane surface in microgravity. The theory is able to accommodate both spatial and temporal variations in the temperature and velocity fields in the liquid surrounding the bubble as it grows. Utilising the present theory, the complicated thermal and hydrodynamic interactions between the vapour, liquid and solid have been manifested for a single isolated bubble growing on a heated plane surface from inception.

1. Introduction

The increased rate of heat transfer during nucleate boiling is determined by the vapour bubbles which grow and depart from the heated surface. Energy is introduced into the liquid by conduction from the heated solid surface and is stored within a thin thermal boundary layer adjacent to the surface. During surface boiling, this energy is ultimately used to vaporise the liquid and cause bubbles to form and grow. Furthermore, fluid motions induced by bubble growth disrupt the thermal boundary layer, thus enhancing the local rate of heat transfer. Consequently, insight into the mechanisms which are responsible for transporting energy away from a heated surface can be gained by understanding the nature of bubble growth.

Early theoretical works focussed on the ideal case of spherically symmetric bubble expansion in a uniformly superheated infinite pool of liquid. With these simplifications, the rate of bubble growth is determined by the surface tension, the liquid inertia and the difference in pressure between the vapour within the bubble and the ambient liquid. Analytic expressions which fully describe the growth of a bubble were unattainable because of the complicated thermal and hydrodynamic interaction of the vapour and liquid at the bubble wall. This was further complicated by coupling between the liquid momentum and energy equations through the non-linear convection term. To reduce the complexity of the problem, Rayleigh [1], Plesset and Zwick [2] and Forster and Zuber [3] considered two limiting regions of bubble growth separately. Lord Rayleigh [1] solved the one-dimensional problem by considering the case in which growth or collapse is governed by momentum interaction between the bubble and ambient fluid. This later became known as the *inertia controlled* stage of bubble growth. Almost four decades later, Plesset and Zwick [2] and Forster and Zuber [3] independently determined that the later stage of bubble growth is controlled by the rate at which energy is transferred through the liquid to the vapour–liquid interface. This was termed the *diffusion* or *heat transfer controlled* growth stage. By approximating a solution to the energy equation, it was shown that their first-order solutions were in good agreement with the experimental results provided by Dergarabedian [4] for water with low superheats at atmospheric pressure. Including the effects of radial convection in the liquid, Scriven [5] obtained an expression for the bubble growth rate which is very similar to that of Plesset and Zwick [2] and Forster and Zuber [3].

* Corresponding author. Tel.: +1-905-525-9140; fax: +1-905-572-7944.

E-mail address: juddr@mcmaster.ca (R.L. Judd).

0017-9310/01/$ - see front matter
PII: S0017-9310(00)00294-5

Nomenclature

A	area
D_j	radial grid line
d	distance from vapour–liquid interface
g	earth gravity
g_∞	gravity in which experiments were performed
h_{fg}	latent heat of evaporation
J	Jacobian
k	thermal conductivity
M	grid parameter
N	grid parameter
P	pressure
Q	energy required for bubble growth
q''	heat flux
r	radial direction
r_b	radial coordinate location of bubble interface
R	bubble radius
R_c	initial bubble radius
S_R	grid clustering coefficient
t	time
t^*	time to nucleation
T	temperature
u	radial velocity (spherical coordinates)
U	radial velocity (cylindrical coordinates)
U^c	contravarient velocity
V	axial velocity
V^c	contravarient velocity
z	axial direction
z_b	axial coordinate location of bubble interface

Greek symbols

α	thermal diffusivity
γ	angle measured from z-axis
ε	transformed computational coordinate
η	transformed computational coordinate
ν	kinematic viscosity
ρ	density
τ	transformed computational time

Subscripts

l	liquid
R	at bubble interface
v	vapour
w	wall
1D	one-dimensional
∞	far field

By assuming that the bubble growth rate was bounded by the analytic solutions of Rayleigh [1] for small values of time and that of Plesset and Zwick [2] as time approached infinity, a general relationship was derived by Mikic et al. [6] for spherical bubble growth in a uniformly superheated liquid which involved both the inertia and heat transfer controlled growth stages. This theory was found to be in good agreement with the experimental data of Lien [7] for water over a wide range of system pressures.

Numerical computations of vapour bubble growth in an infinite, uniformly superheated liquid have been performed by Theofanous et al. [8], Judd [9], Board and Duffy [10], Dalle Donne and Ferranti [11], and Lee and Merte [12]. In the first three works, approximate solutions to the energy equation were used, whereas in the latter two works, a more rigorous numerical solution of the entire energy equation, including the non-linear convective term, was obtained.

The mechanisms associated with vapour bubble growth at a plane heated surface are not understood nearly as well as unbounded growth in an infinite pool. This is due to the fact that it is exceedingly difficult to control the temperature and flow field in the vicinity of growing bubbles during experimental investigations due to natural convection and liquid motions induced by other bubbles. Due to the rapidly varying temperature and flow fields, large scatter is observed in the available bubble growth data at earth gravity, which makes comparison with theory very difficult because of the uncertainty involved in matching the initial and boundary conditions.

However, recent data have been reported by Lee [13], Lee and Merte [14], and Merte et al. [15], in which the shortcomings associated with earth gravity surface boiling experiments are partially overcome by heating a stagnant pool of liquid to the onset of boiling in microgravity. The absence of any significant natural convection, combined with the fact that, during the early stages of growth, the thermal and flow fields are not influenced by previous or neighbouring bubbles, provide well-defined initial and boundary conditions. Even still, the temperature distribution in the solid and liquid were not measured directly, so that approximations are required for determining the initial liquid temperature field and the boundary condition for the solid heater. A further simplification results from the fact that, for some of the measurements, the bubble remained nearly hemispherical for a significant portion of the growth period. The fixed bubble shape adds considerable simplification with respect to theoretical modelling and an accompanying solution procedure. In this manner, Lee and Merte [14] and Merte et al. [15] were able to compare the experimental hemispherical bubble growth data, obtained in R113 on a flat solid surface subject to transient heating, with the theoretical predictions of two one-dimensional spherical models. In the first, an initial uniform liquid temperature, equal to the highest surface

temperature which occurs at nucleation, was assumed. This represented the upper bound on the bubble growth rate, since the highest temperature was assumed to exist everywhere throughout the liquid. The second model assumed a spherically symmetric, non-uniform temperature field around the bubble. The temperature distribution was assumed to be identical to that occurring normal to the heated surface at nucleation. This was regarded as the 'minimum temperature distribution' and represented the lower bound on the bubble growth rate. All of the measured growth curves presented in [13–15] fell between bounds defined by the uniform and non-uniform models.

This paper describes the development of a two-dimensional theoretical model which is capable of predicting both spherically symmetric vapour bubble growth in an infinite pool of liquid as depicted in Fig. 1(a) and hemispherical vapour bubble growth at a heated plane surface as depicted in Fig. 1(b). The theory is the logical progression from the work provided in [13–15] in that it can incorporate either a one-dimensional radially symmetric or a two-dimensional spatially distributed liquid temperature field. It must be carefully noted that the applicability of the present model is limited to the special case in which the energy utilised by the bubble as it grows is supplied by the superheated liquid layer which surrounds the bubble cap. Any contribution of an evaporating microlayer at the base of the bubble to the net mass transfer rate into the bubble, or its influence on the thermal field in the solid during heterogeneous bubble growth, is wholly disregarded. The purpose of this investigation is twofold. First, to advance a simplified physical model and solution procedure for heterogeneous bubble growth. Because many of the fundamental mechanisms are the same, study of this simplified type of growth provides a starting point for more complex theoretical development. Second, to elucidate the factors which contribute to bubble growth.

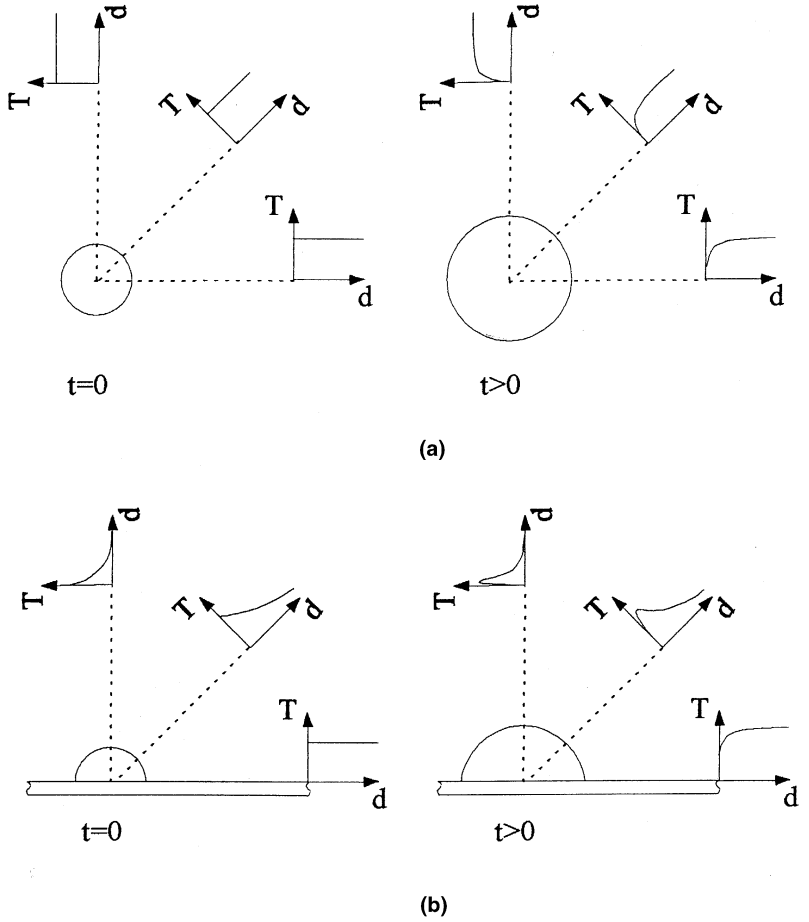

Fig. 1. (a) Spherical vapour bubble growth in an unbounded liquid with a uniform temperature field at $t = 0$ and a spherically symmetric temperature profile for $t > 0$; (b) hemispherical vapour bubble growth at a heated flat surface with a non-uniform temperature field at $t = 0$ and a spherically non-symmetric temperature profile for $t > 0$.

By considering a significant portion of the growth period of a single isolated bubble beginning from inception, the proportional contributions of the various mechanisms which govern growth can be discerned.

2. Formulation of the problem

Fig. 2 shows a sketch of the hemispherical vapour bubble growing at a heated plane surface. Although a viscous boundary layer is known to exist in the liquid above the heated surface, in most practical applications this layer is very thin compared with the size of the bubble so that its overall influence on the bubble as is grows can be neglected. This, coupled with the impermeable wall boundary condition, allows for liquid flow symmetry to be assumed about the r-axis. As a result, hemispherical bubble growth can be modelled as a half segment of the spherical case. In doing so, the equation of motion for the radius, R, of the hemispherical vapour bubble is approximated by the equation for a growing sphere given by

$$P_v(T_v) - P_\infty = \rho_l R\frac{d^2R}{dt^2} + \frac{3}{2}\rho_l\left(\frac{dR}{dt}\right)^2 + \frac{2\sigma}{R}. \tag{1}$$

Eq. (1) is the extended Rayleigh equation which represents a force–momentum balance between the bubble and surrounding liquid. A detailed derivation of this relationship can be found in Riznic et al. [16]. The initial bubble radius is determined by assuming that the vapour is initially saturated, with $T_v = T_\infty$, and that it exists in unstable equilibrium with the quiescent surroundings. For a stationary vapour bubble with internal pressure $P_{sat}(T_v)$ at equilibrium with a liquid at pressure P_∞, the Young–Laplace equation gives an initial radius of,

$$R_c = \frac{2\sigma}{P_{sat}(T_v) - P_\infty}. \tag{2}$$

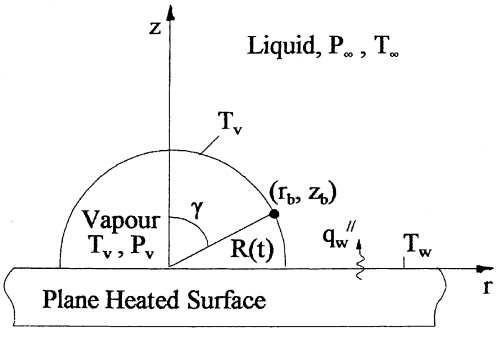

Fig. 2. Hemispherical bubble growing on a plane heated surface.

As a result of the dependence of the vapour pressure on temperature, at least one more equation is required to fully describe this type of bubble growth problem. This expression is obtained by considering an energy balance at the vapour–liquid interface. The energy, Q, required to expand the bubble is supplied by molecular conduction across the thin thermal boundary layer that exists in the liquid around the bubble. Therefore, the rate of change in the energy contained in the vapour bubble is such that

$$\frac{dQ}{dt} = \int_{A_S} k_l\left(\frac{\partial T}{\partial n}\right)_R dA, \tag{3}$$

where A_S is the surface area of the bubble and $(\partial T/\partial n)_R$ is the temperature gradient normal to the interface. Various researchers [1,3,5,10,11] propose different formulations for the term dQ/dt. However, for commonly used fluids well below the critical pressure, the interfacial energy balance can be reduced to

$$h_{fg}\rho_v\frac{dR}{dt} + h_{fg}\frac{R}{3}\frac{d\rho_v}{dt} = \frac{1}{2\pi R^2}\int_{A_S} k_l\left(\frac{\partial T}{\partial n}\right)_R dA. \tag{4}$$

In the above expression, the vapour motion and property variations within the bubble are neglected. Riznic et al. [16] provide a comprehensive derivation of Eq. (4).

Typically, during nucleate pool boiling, energy is continually supplied to the liquid by heat transfer normal to the plane heated surface throughout the entire growth interval of the bubble. Furthermore, an initial liquid temperature distribution which is spherically symmetric around the bubble is not common for most practical boiling applications. These two conditions introduce two-dimensional effects which need to be accounted for in order to adequately describe this type of bubble growth. As a result, the temperature gradient at the bubble wall is obtained by numerically solving the two-dimensional energy equation in axisymmetric cylindrical coordinates for the moving liquid,

$$\frac{\partial T}{\partial t} + U\frac{\partial T}{\partial r} + V\frac{\partial T}{\partial z} = \alpha_l\left(\frac{\partial^2 T}{\partial r^2} + \frac{1}{r}\frac{\partial T}{\partial r} + \frac{\partial T}{\partial z}\right), \tag{5}$$

with initial and boundary conditions given by

$$\begin{aligned} &T(r,z,0) = T_0(r,z),\\ &T(r_b,z_b,t) = T_v,\\ &T(\infty,\infty,t) = T_{1D}(z,t),\\ &\frac{\partial T}{\partial r}(0,z,t) = 0,\\ &\frac{\partial T}{\partial z}(r,0,t) = \frac{q''_w}{k_l}. \end{aligned} \tag{6}$$

The initial condition requires the entire temperature field in the liquid to be specified. A zero flux boundary

condition is assumed at the symmetry boundary (z-axis) and a constant heat flux boundary condition is established at the plane heated surface (r-axis). Some discussion is warranted concerning the assumption of a constant and uniform heat flux at the solid–liquid interface. Admittedly, this assumption significantly reduces the complexity of the problem by eluding the solution of the energy equation in the solid. However, Gau and El-Genk [17] showed that a constant heat flux can be a reasonable approximation for the case in which energy is supplied to the liquid by resistance heating of a thin metallic coating deposited on a glass substrate, so long as the layer is thin enough to restrict the lateral flow of heat through the metal coating. For the experiments presented in [13–15] a 400 Å transparent gold film was deposited on a polished glass substrate. The thinness of the metallic layer precludes any significant lateral heat flow so that a constant heat flux boundary condition is an adequate representation of the surface for comparison with this data. A third boundary condition is obtained by assuming that the vapour phase is lumped and that the temperature of the liquid at the interface is identical to the temperature of the vapour. Finally, the far-field boundary condition is approximated from the analytic solution for one-dimensional axial conduction in a semi-infinite medium. The axial and radial velocities are determined as functions of the instantaneous bubble radius and interface velocity by assuming that the flow field can be determined by the solution for potential flow around an expanding sphere in an unbounded liquid. The velocity components are

$$U = \frac{\mathrm{d}R}{\mathrm{d}t}\left(\frac{R}{(r^2+z^2)^{1/2}}\right)^2 \sin(\gamma),$$
$$V = \frac{\mathrm{d}R}{\mathrm{d}t}\left(\frac{R}{(r^2+z^2)^{1/2}}\right)^2 \cos(\gamma). \tag{7}$$

A brief description of the finite difference solution of the energy equation is set out in Appendix A.

Finally, it is postulated that the vapour is saturated and remains so throughout the bubble growth interval. In this way, the vapour pressure and density can be specified as functions of the saturated vapour temperature,

$$P_\mathrm{v}(T_\mathrm{v}) = a_1 T_\mathrm{v} + a_2 T_\mathrm{v}^2 + a_3 T_\mathrm{v}^3 + a_4 T_\mathrm{v}^4 + a_5 T_\mathrm{v}^5,$$
$$\rho_\mathrm{v}(T_\mathrm{v}) = c_1 T_\mathrm{v} + c_2 T_\mathrm{v}^2 + c_3 T_\mathrm{v}^3 + c_4 T_\mathrm{v}^4 + c_5 T_\mathrm{v}^5. \tag{8}$$

As in [12–14], the property variations with temperature are obtained from a fifth-order polynomial representation of the available property data. With these simplifications, only the rate of change of one state variable, in this case temperature, need be considered given that

$$\frac{\mathrm{d}P_\mathrm{v}}{\mathrm{d}t} = \left(\frac{\mathrm{d}P_\mathrm{v}}{\mathrm{d}T_\mathrm{v}}\right)\frac{\mathrm{d}T_\mathrm{v}}{\mathrm{d}t},$$
$$\frac{\mathrm{d}\rho_\mathrm{v}}{\mathrm{d}t} = \left(\frac{\mathrm{d}\rho_\mathrm{v}}{\mathrm{d}T_\mathrm{v}}\right)\frac{\mathrm{d}T_\mathrm{v}}{\mathrm{d}t}. \tag{9}$$

3. Solution procedure

Eqs. (8) and (9) together with Eqs. (1) and (4) form a set of simultaneous equations for the four unknowns T_v, P_v, ρ_v and R, which were solved numerically using a fourth-order Runge–Kutta method. In order to initiate bubble growth, the equilibrium radius R_c was perturbed by allowing it to increase by a very small amount over an infinitesimally small time interval. This is equivalent to a disturbance in temperature or pressure [10]. A comprehensive discussion on the initial disturbance can be found in [12] and [13]. For this study, the initial time step never exceeded 10^{-7} s, and the radius increase did not exceed 0.05% of the initial radius. Care was taken to ensure that the magnitude of the initial disturbance did not significantly affect the computed growth curve.

4. Comparison with experiment

4.1. Spherical bubble growth

A wealth of experimental data exists for spherical bubble growth in liquids with an initial uniform superheat. This, coupled with the fact that many of the more complex features of heterogeneous growth are absent during homogeneous growth, provides a good test for the present theory and computational procedure. To investigate spherically symmetric growth, the initial

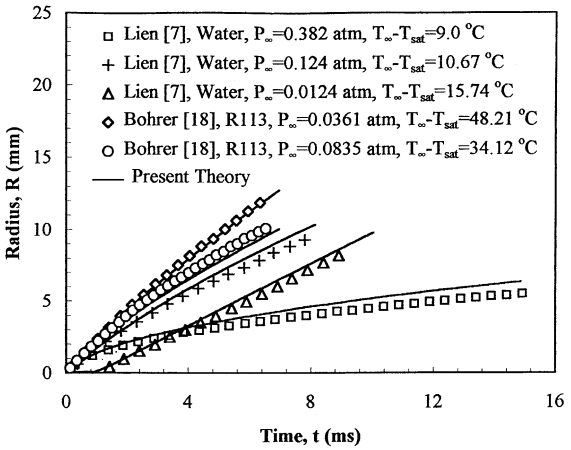

Fig. 3. Comparison of computed results with experimental data for spherical bubble growth in water and refrigerant R113.

temperature distribution is set to be spatially uniform, and symmetry about the r-axis is approximated by setting $q''_w = 0$ to establish a zero temperature gradient.

Fig. 3 shows the comparison of the predictions of the present theory with experimental data of Lien [7] and Bohrer [18]. In the figure, the present theory shows acceptable agreement with the experimental data for homogeneous bubble growth for a range of system pressures and initial liquid superheats for two different fluids. Similar agreement was observed with the bubble growth data provided by Dergarabedian [4] and Board and Duffy [10] for superheated water.

4.2. Hemispherical bubble growth

Heterogeneous bubble growth depends strongly on the amount of energy stored in the thermal boundary layer which forms adjacent to the heater surface. The sensible heat stored in the liquid is converted to latent heat by evaporation into the bubble as it grows. As a result, any predictive model of bubble growth requires that the temperature profile in the liquid be known prior to bubble growth. By heating a quiescent, uniform temperature liquid in microgravity, Lee [13] was able to show that the solution of the one-dimensional transient heat conduction equation for a constant heat flux boundary condition in a semi-infinite solid did a very good job at predicting the measured mean surface temperature. Consequently, the initial temperature distribution in the liquid could be predicted by the expression

$$T(z,t^*) = T_\infty + \frac{2q''_w\sqrt{\alpha_l t^*/\pi}}{k_l}\exp\left(-\frac{z^2}{4\alpha_l t^*}\right) - \frac{q''_w z}{k_l}\operatorname{erfc}\left(\frac{z}{\sqrt{4\alpha_l t^*}}\right), \tag{10}$$

where t^* is the time to the onset of boiling. This expression, together with the assumption of a quiescent liquid, specifies the initial conditions required by the present theory.

Bubble growth predictions for three different test cases are shown in Fig. 4. For each experiment the computational predictions of the two one-dimensional spherically symmetric models, which represent the upper and lower bounds of growth, are given together with the two-dimensional heterogeneous model. As expected, the fully two-dimensional model predicts growth curves

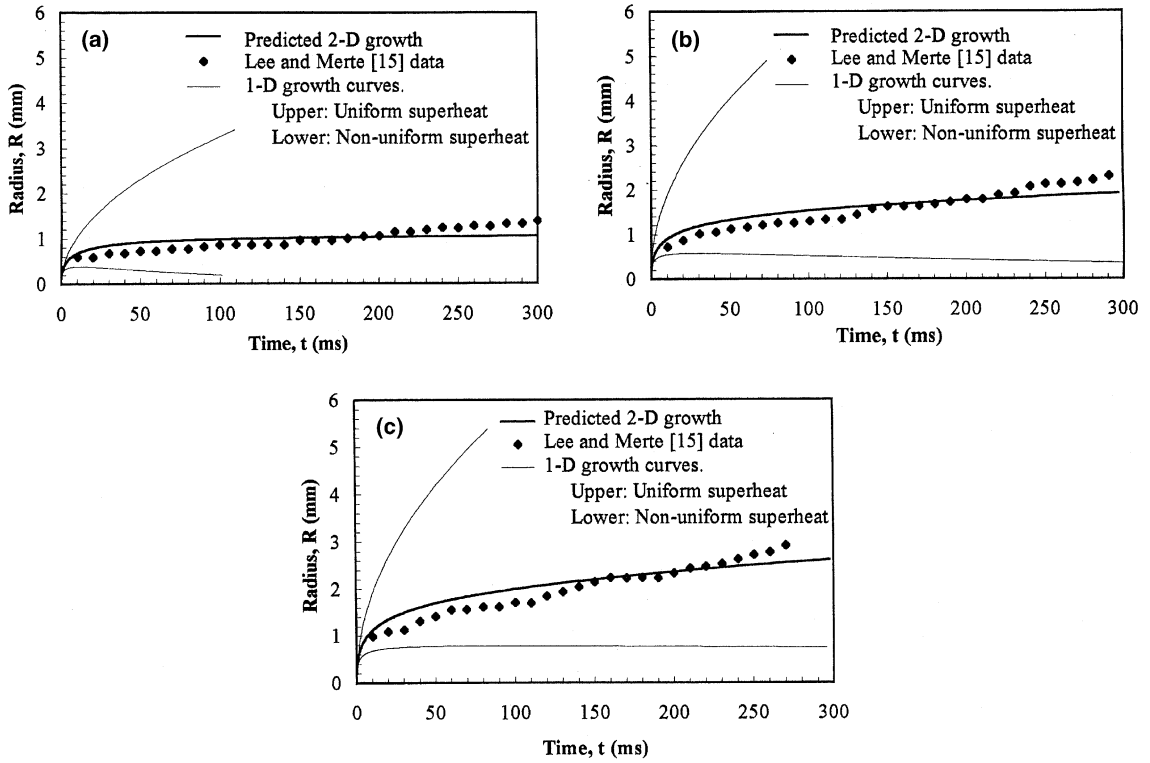

Fig. 4. Comparison of computed results with experiments for hemispherical bubble growth of R113 on a heated plane surface in microgravity, $g_\infty/g = 10^{-4}$ (a) $q'' = 7$ W/cm^2, $P_\infty = 149.9$ kPa, $T_{sat} = 59.8$°C, $T_\infty = 48.3$°C, $t^* = 0.91$ s, $T^*_w = 85.8$°C; (b) $q'' = 6.5$ W/cm^2, $P_\infty = 117.3$ kPa, $T_{sat} = 52$°C, $T_\infty = 48.8$°C, $t^* = 0.74$ s, $T^*_w = 86.3$°C; (c) $q'' = 6.95$ W/cm^2, $P_\infty = 106.8$ kPa, $T_{sat} = 49.1$°C, $T_\infty = 48.35$°C, $t^* = 0.75$ s, $T^*_w = 84.1$°C.

which are positioned somewhere inbetween the upper and lower bounds as depicted in the figure. More importantly, satisfactory agreement is observed between the measured growth curves over a large portion of the respective growth intervals. This lends support to the physical modelling of the problem as well as the numerical techniques utilised in the computations. It can be noted that the agreement between the computed and experimental curves lends support to the assumption that, for these specific test cases, microlayer evaporation did not play a significant role in the bubble growth process.

5. Bubble dynamics

In the following sections, the growth characteristics of a single isolated hemispherical bubble growing at a plane heated surface with negligible effect of an evaporating microlayer will be discussed. The boiling conditions are identical to those of Fig. 4(b). Fig. 5 shows the time variation of the predicted bubble radius and vapour temperature. In the figure, four regions of growth have been demarcated and will be discussed in turn. In Fig. 6 the energy equation for the vapour bubble, Eq. (4), has been decomposed to expose the time varying contributions of its constituent terms. From the figure, it is apparent that the term involving the rate of change of vapour density $(1/3)h_{fg}R(d\rho_v/dt)$, is negligible compared with the interface velocity term, $h_{fg}\rho_v(dR/dt)$. Thus, for discussion purposes, the growth rate can be considered proportional to the area averaged heat flux into the bubble throughout its growth,

$$\frac{dR}{dt} \propto \frac{1}{A_S}\int_{A_S} k_l\left(\frac{\partial T}{\partial n}\right)_R dA = q''_{ave}. \tag{11}$$

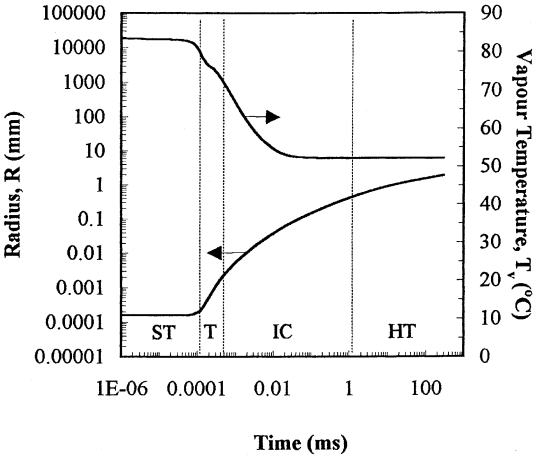

Fig. 5. Bubble radius (R) and temperature (T_v) histories for hemispherical bubble growing atop a heated surface.

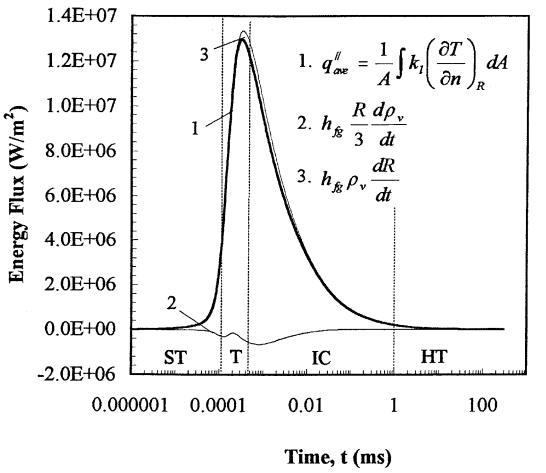

Fig. 6. Decomposition of the energy equation, Eq. (4), showing four growth domains: surface tension controlled (ST), transition (T), inertial controlled (IC), and heat transfer controlled (HT).

In Fig. 7, the constituent components of the equation governing the motion of the interface, Eq. (1), are represented. In the figure, the pressure difference, $P_v - P_\infty$, is balanced by the stress in the interface through the surface tension term, $2\sigma/R$, and the hydrodynamic pressure, P_{hd}, defined as

$$P_{hd} = \rho_l R\frac{d^2R}{dt^2} + \frac{3}{2}\rho_l\left(\frac{\partial R}{\partial t}\right)^2. \tag{12}$$

The hydrodynamic pressure can be regarded as the excess pressure at the bubble interface that is a direct consequence of the bulk motion of the liquid. The total pressure in the liquid at the interface is related to the hydrostatic and hydrodynamic pressures through $P_R = P_\infty + P_{hd}$.

5.1. Surface tension controlled growth (ST)

During the surface tension controlled domain, energy is continuously supplied to the bubble by conduction through the liquid. This is evident from the positive value of q''_{ave} in Fig. 6. However, the average heat flux into the bubble, and thus the growth rate dR/dt, are small enough that the contribution of the hydrodynamic pressure in balancing the equation of motion is insignificant so that it essentially reduces to a static force balance, $P_v - P_\infty \approx 2\sigma/R$, as shown in Fig. 7(a). Because P_∞ is constant, an increase in the bubble radius must occur in conjunction with a decrease in P_v, which of course coincides with a proportional decrease in the vapour temperature, T_v. This is an important effect because the decreasing vapour temperature represents a decreasing interface boundary temperature for the liquid.

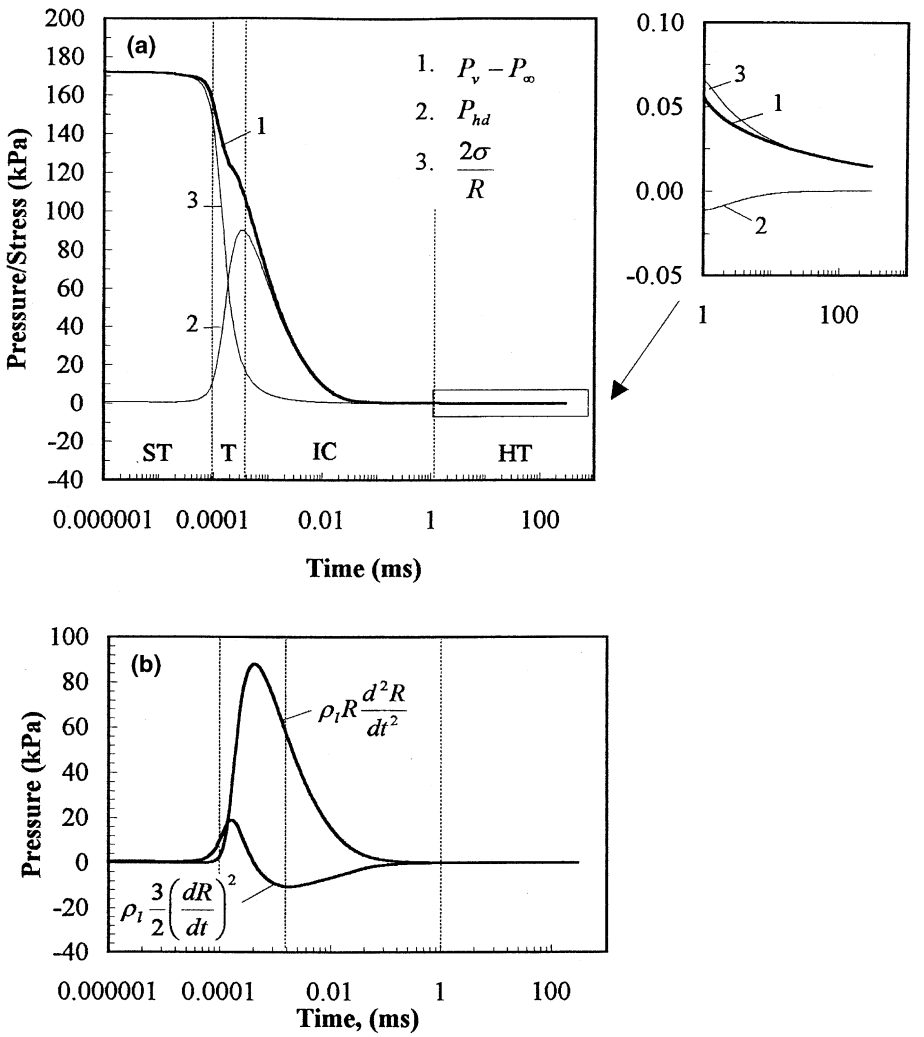

Fig. 7. (a) Decomposition of the equation of motion, Eq. (1) showing the four growth domains: surface tension controlled (ST), transition (T), inertial controlled (IC), and heat transfer controlled (HT); (b) constituent terms of the hydrodynamic pressure term given in Eq. (12).

As the liquid is essentially still, the decreasing interfacial liquid temperature acts to increase the interfacial temperature gradient, $(\partial T/\partial n)_R$. The magnitude of the temperature gradients at the interface can be characterised by considering the tip and base of the bubble as the bounding values. These are shown in Fig. 8. It can thus be said that bubble growth in this domain is accelerated due to a positive feedback effect in which the increase in the radius, R, is related to a decreasing interfacial liquid temperature. This corresponds with an increase in q''_{ave}, through the increase in the magnitude of the local temperature gradient, which feeds back by a proportional increase in the bubble growth rate, dR/dt. In the earliest stage of the surface tension domain, this feedback effect is not significant. However, in the latter stage, it becomes appreciable as indicated by a noticeable increase in R away from R_c (Fig. 5), a significant decrease in both T_v and P_v (Figs. 5 and 7(a), respectively) and a sharp rise in q''_{ave} (Fig. 6)

5.2. Transition domain (T)

As the bubble interface is accelerating radially outward there comes a point at which the effects of the bulk liquid motion outside the bubble are no longer insignificant. The transition domain is thus distinguished from the surface tension domain by the relative contributions of the surface tension term and the hydrodynamic pressure term in balancing the equation of motion. Fig. 7(a) shows that the excess pressure at the

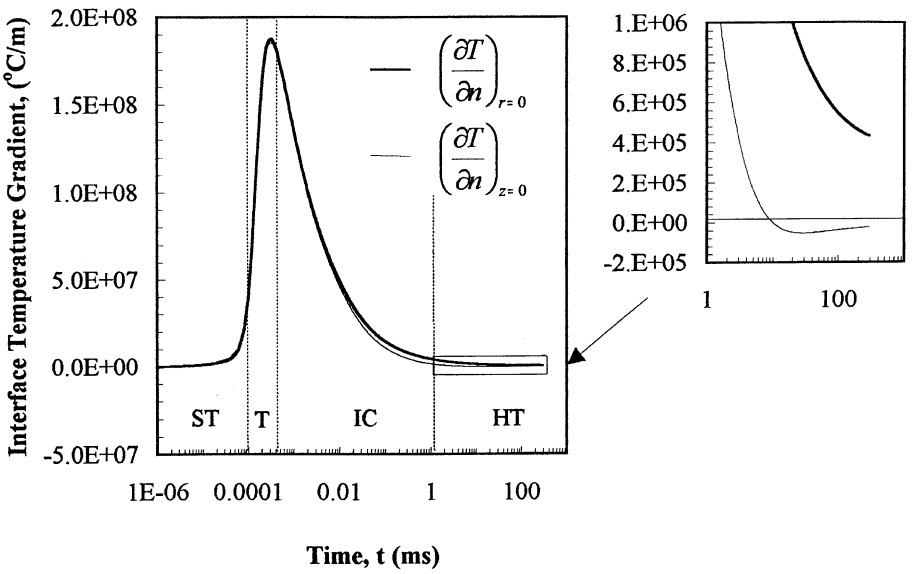

Fig. 8. Interfacial liquid temperature gradient histories at the top of the hemispherical bubble (along z-axis), and the base of the hemispherical bubble (along r-axis).

interface due to flow effects, P_{hd}, rises sharply at the beginning of this region and quickly becomes of the same order of magnitude as the surface tension term, $2\sigma/R$.

At the beginning of the transition domain the effects of liquid motions are still small, so that both q''_{ave} and dR/dt continue to increase rapidly as a result of the positive feedback effect discussed earlier. However, as evident from Fig. 6, the rate of change of q''_{ave} and dR/dt are shown to decrease in the latter stage and reach a maximum value at approximately 3×10^{-4} ms. Because the decreasing vapour temperature tends to have a positive influence on the local temperature gradient and thus q''_{ave}, this signifies that there are mechanisms at work which tend to oppose the increase of q''_{ave}. The most obvious is the fact that, as the growing bubble faces the additional resistance associated with forcing the bulk liquid out radially, the rate at which P_v and T_v decrease becomes less rapid. This tends to adversely affect the rate at which $(\partial T/\partial n)_R$ and q''_{ave} increase. The significant decrease in the slopes are demarcated by the 'inflection' on the T_v and $P_v - P_\infty$ curves shown in Figs. 5 and 7(a), respectively. Secondly, conduction and advection occur in the liquid adjacent to the interface. Each of these heat transfer mechanisms act in such a way as to diminish the temperature gradients in the immediate vicinity of the vapour–liquid interface and thus have a detrimental influence on the rate at which q''_{ave} and dR/dt increase. Advection describes the mechanism by which thermal energy is transported into the bulk of the liquid away from the bubble interface due to outward radial flow. Conduction, on the other hand, is responsible for the transport of energy into the vapour bubble, and to a lesser extent into the bulk liquid. This is illustrated in Fig. 9, where the temperature profiles along the z- and r-axes are shown.

5.3. Inertial controlled growth (IC)

Inertia controlled growth refers to the interval of bubble growth in which the rate of bubble expansion is considered to be limited by the rate at which the growing interface can push back the surrounding liquid [19]. In this domain, the average heat flux into the bubble is very high, as illustrated in Fig. 6, so that heat transfer to the interface is not the limiting mechanism of growth.

Fig. 7(a) shows that the pressure difference, $P_v - P_\infty$, is now balanced by the hydrodynamic pressure at the interface. The hydrodynamic pressure comprises two 'inertial' terms as given in Eq. (12). These are the acceleration term, $\rho_l R(d^2R/dt^2)$, and the velocity term, $(3/2)\rho_l(dR/dt)^2$. These are plotted in Fig. 7(b). The two terms are of differing sign and thus tend to have an opposite influence on the total liquid pressure, and thus the force of the liquid on the bubble interface. The negative acceleration term accounts for the fact that the fluid body surrounding the bubble is decelerating, causing outward force on the bubble surface. The velocity term is positive because the expanding bubble wall is effectively pushing the fluid outwardly. The reaction force of the liquid on the bubble wall is thus inwardly directed and must be of opposite sign.

This inertial controlled growth domain is characterised by a decreasing average heat flux and decelerating

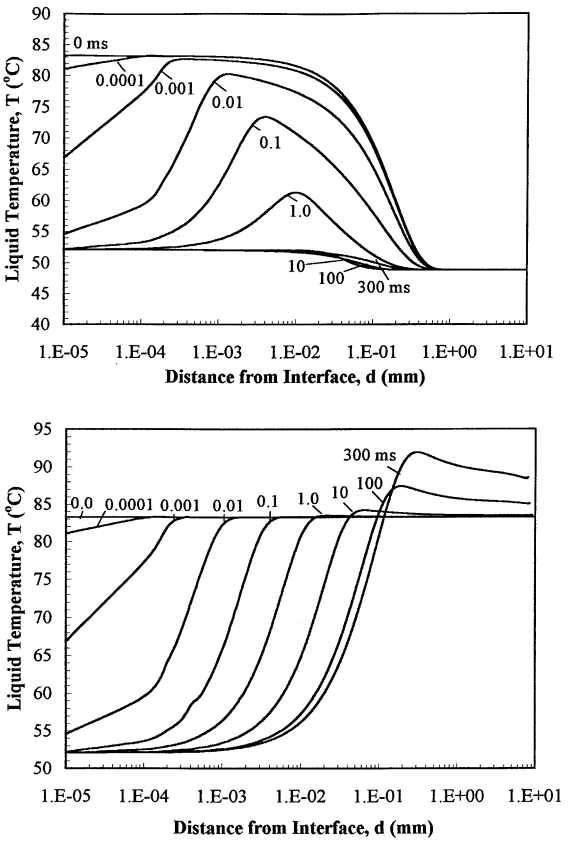

Fig. 9. Computed liquid temperature distribution at (a) the top of the hemispherical bubble (along z-axis), and (b) the base of the hemispherical bubble (along r-axis) at various times.

interface as shown in Fig. 6. This signifies that the positive influence that the decreasing vapour temperature tends to have on the local temperature gradient is not sufficient to compensate for the rate at which advection and conduction serve to decrease the temperature gradient at the interface. Figs. 5 and 8 show that the decreasing vapour temperature occurs in conjunction with decreasing interfacial temperature gradients at the tip and base of the bubble. Fig. 9(a) shows this point more clearly. Here, the interfacial liquid temperature is decreasing. However, due to a net loss of thermal energy by conduction out of the liquid and into the vapour bubble, coupled with conduction and advection of thermal energy away from the bubble and into the bulk liquid, the maximum temperature within the boundary layer decreases and moves further out from the bubble interface. This 'shrinking' and 'stretching' of the thermal boundary layer results in an overall decrease in magnitude of the interfacial temperature gradient, even with a decreasing interfacial liquid temperature. Fig. 9(b) shows a similar effect at the base of the bubble except that the maximum temperature, which is equal to the temperature of the liquid adjacent to the plane heated surface, remains approximately constant during this domain.

5.4. Heat transfer controlled growth (HT)

Heat transfer controlled growth refers to the interval of bubble growth in which the rate of bubble expansion is considered to be limited by the rate at which liquid is evaporated into the bubble, which is dictated by the rate of heat transfer by conduction through the liquid [19]. In this late stage of bubble growth, the interface velocity has slowed enough so that the hydrodynamic pressure, P_{hd}, becomes insignificant compared with the surface tension term, $2\sigma/R$, in balancing the pressure difference, $P_v - P_\infty$. This is shown in Fig. 7(a). As a result, the equation of motion is essentially reduced to a balance of static forces acting at the vapour–liquid interface, $P_v - P_\infty \approx 2\sigma/R$, in much the same way as it did in the surface tension controlled region. However, in contrast with the surface tension controlled region, increases in R do not produce an appreciable decrease in the vapour temperature of the bubble. As shown in Figs. 5 and 9, the vapour temperature remains relatively constant and approximately equal to its minimum value corresponding with the saturation temperature of the system ($T_{v,min} \approx T_{sat}(P_\infty) = 52.0°C$). Because the liquid temperature at the interface is now constant, the positive feedback effect, responsible for the rapid acceleration of the vapour–liquid interface in the surface tension controlled region, does not occur in this domain of growth. Conversely, the 'shrinking' and 'stretching' of the thermal layer in the liquid due to conduction and advection are responsible for the continuous deceleration of the interface due to the diminishing interfacial temperature gradients. The decrease in the growth rate is compounded by the fact that for $t > 10$ ms the top portion of the bubble penetrates into a region of liquid which is subcooled. This point is illustrated in Figs. 8 and 9(a) by the negative value of the interface temperature gradient for the tip of the bubble. Hence from this time onward, the net energy transfer into the bubble is the difference between that which leaves by condensation and that which enters by evaporation.

It is interesting to note that the maximum temperature in the liquid along the heated surface exceeds that of the far field wall temperature. This is illustrated for $t \geqslant 1.0$ ms in Fig. 9(b). At any point along the heated surface there are three heat transfer mechanisms which act together to transport the imposed heat flux: radial conduction tangent to the heater surface, axial conduction normal to the heater surface, and convection due to the flow of liquid over the surface. The lower temperature in the immediate vicinity of the bubble indicates that the imposed heat flux is being transported away from the surface very efficiently. This region is charac-

terised by a relatively high evaporative heat flux into the bubble together with significant convective heat transfer because it is the region of highest liquid velocity. Moving further away from the interface, the influence of evaporation becomes less and the contribution of convective heat transfer decreases due to the rapidly diminishing liquid velocity ($U(r,0,t) \propto 1/r^2$). The surface temperature increases as the less efficient mode of axial conduction normal to the surface becomes an important mode of heat transfer. One might expect the surface temperature to increase asymptotically to the surface temperature in the undisturbed region at R_∞. However, it is evident from interferometric investigations on growing bubbles that the thermal boundary layer thickness adjacent to the surface can be largest near the bubble and decreases at distances further away [20]. Consequently, in order that axial conduction can accommodate the imposed surface heat flux, the surface temperature must be higher in the region of the thicker boundary layer nearer the interface. This is consistent with the observed overshoot in the liquid temperature profile at the heated surface.

6. Conclusions

In recent years, theoretical developments in nucleate pool boiling have been focussed on isolated bubble growth upon a heated surface. It is hoped that an understanding of the mechanisms which determine the growth of bubbles will offer insight into and perhaps predictions of the increased heat transfer coefficient observed in nucleate pool boiling. However, advances in the state of the art are inhibited by the apparent stochastic nature of boiling due to the rapidly varying thermal and flow fields. As a result of the overwhelming complexities, sufficient testing of the physical modelling and computational procedures has not been afforded in the past.

The present theory overcomes this shortcoming in two ways. First, the theory is simple enough to facilitate comparison with data for homogeneous growth in an unbounded fluid. Second, the theory can accommodate the added complexities of a heated surface and time varying spatially distributed liquid temperature fields for hemispherical bubble growth in microgravity. Overall agreement between the present theory and experimental data is very good, which instills confidence in the physical modelling of the problem as well as the computational procedure which has been utilised.

The complicated thermal and hydrodynamic interactions between vapour, liquid and solid have been manifested for a single, isolated bubble growing on a heated plane surface from inception with the negligible contribution of an evaporating microlayer. It has been shown that early bubble growth away from the initial radius is restricted by surface tension forces within the bubble wall. However, minuscule increases in radius result in an increase in the local interfacial temperature gradients, which facilitates growth by increasing the area-averaged heat flux into the bubble. Eventually, bubble growth becomes impeded by the fact that it now must force the surrounding liquid out radially. The heat flux increases to such an extent that this becomes the limiting factor to growth. Nevertheless, the growth rate must eventually decrease with increasing time as the thermal energy stored within the boundary layer which surrounds the bubble is consumed by the bubble as well as transported away from the bubble by advection into the bulk of the liquid. Eventually the growth rate slows enough so that liquid inertia no longer plays an important role, and the growth rate becomes limited by the rate at which energy can be transported to the interface through the liquid.

Appendix A. Computational technique for the energy equation

Utilising subscript notation to denote partial differentiation with respect to the subscript variable, the energy equation in axisymmetric cylindrical coordinates can be expressed as

$$T_t + UT_r + VT_z = \alpha_l(T_{rr} + r^{-1}T_r + T_z), \tag{13}$$

where U and V are the axial and radial components of the liquid velocity defined in Eq. (7).

The energy equation was solved numerically on a grid which was constructed using an algebraic grid generation technique proposed by Chen et al. [21]. The grid variables in the physical domain are depicted in Fig. 10. Grid clustering near the vapour–liquid interface as well the moving boundary were facilitated by defining the grid such that

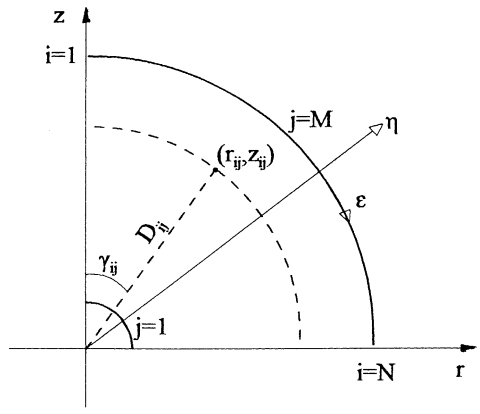

Fig. 10. Grid parameters.

$$r_{ij} = D_j \sin(\gamma_{ij}), \qquad z_{ij} = D_j \cos(\gamma_{ij}), \tag{14}$$

where

$$\gamma_{ij} = \frac{\pi}{2}\left(\frac{i-1}{N-1}\right),$$
$$D_j = 1 + (R_\infty - 1)\left(1 - S_R \tan^{-1}\left[\left(1 - \frac{j-1}{M-1}\right)\tan\left(\frac{1}{S_R}\right)\right]\right), \tag{15}$$

and the term S_R determines the percentage of grid points near the interface. In order that conventional finite difference techniques be utilised, the energy equation was transformed to a stationary grid with uniform grid spacing. The transformation is given by

$$r = r(\varepsilon, \eta, \tau), \qquad z = z(\varepsilon, \eta, \tau), \qquad t = \tau \tag{16}$$

such that

$$\begin{aligned} T_r &= J^{-1}(z_\eta T_\varepsilon - z_\varepsilon T_\eta), \\ T_z &= J^{-1}(r_\varepsilon T_\eta - r_\eta T_\varepsilon), \\ T_t &= T_\tau - T_r r_\tau - T_z z_\tau. \end{aligned} \tag{17}$$

By defining the contravariant velocities as

$$\begin{aligned} U^c &= (U - r_\tau) z_\eta - (V - z_\tau) r_\eta, \\ V^c &= (V - z_\tau) r_\varepsilon - (U - r_\tau) z_\varepsilon, \end{aligned} \tag{18}$$

the transformed energy equation becomes

$$\begin{aligned} T_\tau + J^{-1}U^c T_\varepsilon + J^{-1}V^c T_\eta = {} & J^{-2}\alpha_1(aT_{\varepsilon\varepsilon} - 2bT_{\varepsilon\eta} \\ & + cT_{\eta\eta} + dT_\varepsilon + eT_\eta) \\ & + (Jr)^{-1}\alpha_1(z_\eta T_\varepsilon - z_\eta T_\eta), \end{aligned} \tag{19}$$

where J is the Jacobian and the coefficients a through e are related to the metrics and their derivatives through the following:

$$\begin{aligned} J &= z_\eta r_\varepsilon - z_\varepsilon r_\eta, \\ a &= z_\eta^2 + r_\eta^2, \\ b &= r_\varepsilon r_\eta + z_\varepsilon z_\eta, \\ c &= z_\varepsilon^2 + r_\varepsilon^2, \\ d &= J^{-1}(r_\eta \beta_1 - z_\eta \beta_2), \\ e &= J^{-1}(z_\varepsilon \beta_2 - r_\varepsilon \beta_1), \\ \beta_1 &= az_{\varepsilon\varepsilon} - 2bz_{\eta\varepsilon} + cz_{\eta\eta}, \\ \beta_2 &= ar_{\varepsilon\varepsilon} - 2br_{\eta\varepsilon} + cr_{\eta\eta}. \end{aligned} \tag{20}$$

Eq. (19) was discretised using second-order central difference representations of the spatial derivatives and a fully implicit first order representation of the time derivatives. At a given time step, the temperature field was determined using successive over-relaxation (SOR) by lines. For each line the resulting system of algebraic expressions were solved utilising the efficient tri-diagonal matrix algorithm (TDMA).

References

[1] J.W.S. Rayleigh, On the pressure developed in a liquid during the collapse of a spherical cavity, Phil. Mag. 34 (1917) 94–98.

[2] M.S. Plesset, S.A. Zwick, The growth of vapor bubbles in superheated liquid, J. Appl. Phys. 25 (1954) 493–500.

[3] H.K. Forster, N. Zuber, Growth of vapor bubbles in superheated liquid, J. Appl. Phys. 25 (1954) 474–478.

[4] P. Dergarabedian, The rate of growth of vapour bubbles in superheated water, J. Appl. Mech. 20 (1953) 537–574.

[5] L.E. Scriven, On the dynamics of phase growth, Chem. Eng. Sci. 10 (1959) 1–13.

[6] B.B. Mikic, W.M. Rohsenow, P. Griffith, On bubble growth rates, Int. J. Heat Mass Transfer 13 (1970) 657–665.

[7] Y.C. Lien, Bubble growth rates at reduced pressure, D.Sc. thesis, MIT, 1969.

[8] T. Theofanous, L. Baisi, H.S. Isben, H. Fauske, A theoretical study on bubble growth in constant and time-dependent pressure fields, Chem. Eng. Sci 24 (1969) 885–897.

[9] A.M. Judd, Analysis of transient boiling of liquid metals, Brit. J. Appl. Phys . 2 (1969) 261–274.

[10] S.J. Board, R.B. Duffy, Spherical vapour bubble growth in superheated liquids, Chem. Eng. Sci. 26 (1971) 263–274.

[11] M. Dalle Donne, M.P. Ferranti, The growth of vapour bubbles in superheated sodium, Int. J. Heat Mass Transfer 18 (1975) 477–493.

[12] H.S. Lee, H. Merte Jr., Spherical vapour bubble growth in uniformly superheated liquids, Int. J. Heat Mass Transfer 39 (1996) 2427–2447.

[13] H.S. Lee, Vapour bubble dynamics in microgravity, Ph.D. thesis, University of Michigan, 1993.

[14] H.S. Lee, H. Merte Jr., Hemispherical vapour bubble growth in microgravity: experiments and model, Int. J. Heat Mass Transfer 39 (1996) 2449–2461.

[15] H. Merte, Jr., H.S. Lee, R.B. Keller, Report on pool boiling experiment flown on STS-47-57-60, report no. UM-MEAM-95-01, Department of Mechanical Engineering and Applied Mechanics, The University of Michigan, Ann Arbor, MI, NASA contract NAS 3-25812, 1995.

[16] J. Riznic, G. Kojasoy, N. Zuber, On the spherically symmetric phase change problem, Int. J. Fluid Mech. Res. 26 (1999) 110–145.

[17] Z. Gau, M. El-Genk, Liquid microlayer evaporation during nucleate boiling on the surface of a flat composite wall, Int. J. Heat Mass Transfer 37 (1996) 1641–1655.

[18] T.H. Bohrer, Bubble growth in highly superheated liquids, M.S. thesis, Purdue University, 1973.

[19] V.P. Carey, Liquid–Vapor Phase-Change Phenomena, Hemisphere, Washington, DC, USA, 1992.

[20] S. Van Stralen, R. Cole, Boiling Phenomenon, Hemisphere, USA, 1979, p. 833.

[21] W. Chen, R. Mei, J.F. Klausner, Vapor bubble growth in highly subcooled heterogeneous boiling, in: Convective Flow Boiling Conference, paper II-4, 1995.